

AD A109296

NO ETC-102-  
D-FOS DZA EDC-102-  
UN-2A10M3

DTIC FILE COPY

LEVEL

12

IFSM-81-107

LEHIGH UNIVERSITY



SURFACE REACTIONS AND FATIGUE CRACK GROWTH

DTIC  
ELECTED  
JAN 6 1982  
H

by

R. P. Wei and G. W. Simmons

August, 1981

DISTRIBUTION STATEMENT A  
Approved for public release;  
Distribution Unlimited

Technical Report No. 11

Office of Naval Research

Contract N00014-75-C-0543, NR 036-097

82 01 06 003

Unclassified

SECURITY CLASSIFICATION OF THIS PAGE (When Data Entered)

REPORT DOCUMENTATION PAGE		READ INSTRUCTIONS BEFORE COMPLETING FORM
1. REPORT NUMBER IFSM-81-107	2. GOVT ACCESSION NO. 11-4019	3. RECIPIENT'S CATALOG NUMBER 11
4. TITLE (and Subtitle) SURFACE REACTIONS AND FATIGUE CRACK GROWTH		5. TYPE OF REPORT & PERIOD COVERED Technical Report No. 11
7. AUTHOR(s) R. P. Wei and G. W. Simmons		6. PERFORMING ORG. REPORT NUMBER
9. PERFORMING ORGANIZATION NAME AND ADDRESS Lehigh University Bethlehem, PA 18015		8. CONTRACT OR GRANT NUMBER(s) Contract N00014-75-C-0543
11. CONTROLLING OFFICE NAME AND ADDRESS Office of Naval Research Department of the Navy Arlington, VA		10. PROGRAM ELEMENT, PROJECT, TASK AREA & WORK UNIT NUMBERS NR 036-097
14. MONITORING AGENCY NAME & ADDRESS (if different from Controlling Office)		12. REPORT DATE August, 1981
		13. NUMBER OF PAGES 19
		15. SECURITY CLASS. (of this report) Unclassified
		15a. DECLASSIFICATION/DOWNGRADING SCHEDULE
16. DISTRIBUTION STATEMENT (of this Report) This document has been approved for public release and sale; its distribution is unlimited.		
17. DISTRIBUTION STATEMENT (of the abstract entered in Block 20, if different from Report)		
18. SUPPLEMENTARY NOTES		
19. KEY WORDS (Continue on reverse side if necessary and identify by block number) Fracture mechanics, Surface chemistry, Environmental assisted fatigue crack growth, Modeling, Gas mixtures and Corrosion fatigue.		
20. ABSTRACT (Continue on reverse side if necessary and identify by block number) Recent fracture mechanics and surface chemistry studies of environment assisted crack growth in gaseous environments have shown that crack growth may be controlled in some systems by the rate of surface reactions and in others by the rate of transport of the aggressive environment to the crack tip. Based on con- siderations of surface reactions and gas transport, a model for surface reaction and transport controlled fatigue crack growth		

DD FORM 1 JAN 73 1473

EDITION OF 1 NOV 65 IS OBSOLETE  
S/N 0102-014-6601

Unclassified

SECURITY CLASSIFICATION OF THIS PAGE (When Data Entered)

407099

Unclassified

SECURITY CLASSIFICATION OF THIS PAGE(When Data Entered)

in single component gaseous environments was proposed and experimentally verified. In practice, however, there is usually more than one gas in a given environment. The various component gases can compete for surface reaction sites and therefore alter the fatigue crack growth response. In this paper, the development of the model for surface reaction and transport controlled fatigue crack growth in single component gaseous environments is briefly reviewed. Modeling of fatigue crack growth in a binary gas mixture, in which one of the components acts as an inhibitor, is described, and the model is applied to the consideration of the influence of oxygen on fatigue crack growth in humid air.

Accession For	
NTIS	✓
DTIC	
Uncl	
Spec	
By	
Distribution of	
Available to	
For	
Dist	Special

Unclassified

SECURITY CLASSIFICATION OF THIS PAGE(When Data Entered)

**SURFACE REACTIONS AND FATIGUE CRACK GROWTH**

by

**R. P. Wei and G. W. Simmons**  
Lehigh University  
Bethlehem, PA 18015

This document has been approved for public release and  
sale; its distribution is unlimited.

## SURFACE REACTIONS AND FATIGUE CRACK GROWTH

R. P. Wei and G. W. Simmons

Lehigh University  
Bethlehem, PA 18015

### INTRODUCTION

Recent fracture mechanics and surface chemistry studies of environment assisted crack growth in gaseous environments<sup>1-4</sup> have shown that crack growth may be controlled in some systems by the rate of surface reactions and in others by the rate of transport of the aggressive environment to the crack tip. Based on considerations of surface reactions and gas transport, a model for surface reaction and transport controlled fatigue crack growth in single component gaseous environments was proposed and experimentally verified.<sup>5-8</sup> This model is able to account for the influences of gas pressure and cyclic load frequency on the rate of fatigue crack growth. In practice, however, there is usually more than one gas in a given environment. The various component gases can compete for surface reaction sites and therefore alter the fatigue crack growth response. The effect of this competition needs to be considered. In this paper, the development of the model for surface reaction and transport controlled fatigue crack growth in single component gaseous environments is briefly reviewed. Extension of the same considerations to fatigue crack growth in a binary gas mixture, in which one of the components acts as an inhibitor, is described. Quantitative application of this model to the consideration of oxygen on fatigue crack growth in humid air is discussed.

### MODELING OF FATIGUE CRACK GROWTH IN ONE COMPONENT GAS

Modeling of environment assisted fatigue crack growth in single-component gaseous environments was based on the proposition that the rate of crack growth in an aggressive environment,  $(da/dN)_e$ , is

composed of the sum of three components.<sup>5,8,10</sup>

$$(da/dN)_e = (da/dN)_r + (da/dN)_{cf} + (da/dN)_{scc} \quad (1)$$

$(da/dN)_r$  is the rate of fatigue crack growth in an inert environment and, therefore, represents the contribution of "pure" (mechanical) fatigue. This component is essentially independent of frequency at temperatures where creep is not important.  $(da/dN)_{scc}$  is the contribution by sustained-load crack growth (that is, stress corrosion cracking) at K levels above  $K_{Iscc}$ .<sup>11</sup> The contribution by sustained-load crack growth, i.e., the  $(da/dN)_{scc}$  term, has been examined in some detail previously,<sup>11,12</sup> and appears to be adequately accounted for by the superposition model.<sup>11</sup>  $(da/dN)_{cf}$  represents a cycle-dependent contribution requiring synergistic interaction of fatigue and environmental attack, and was not considered by Wei and Landes.<sup>11</sup> This model,<sup>5</sup> therefore, was directed specifically to the cycle-dependent term, and was limited to establishing a formal framework for estimating frequency and pressure dependence of  $(da/dN)_{cf}$  in single-component gaseous environments. (Examinations of the influences of other loading variables (such as, load ratio) are in progress.)

In the model,<sup>5</sup> environmental enhancement of fatigue crack growth is assumed to result from embrittlement by hydrogen that is produced by the reaction of hydrogenous gases (e.g., water vapor) with the freshly produced fatigue crack surfaces. More specifically,  $(da/dN)_{cf}$  is assumed to be proportional to the amount of hydrogen produced by the surface reaction during each cycle, which is proportional in turn to the "effective" crack area<sup>1/</sup> produced during the prior loading cycles and to the extent of surface reaction. The time available for reaction is assumed to be equal to one-half of the fatigue cycle.<sup>5</sup> Transport of gaseous environments to the crack tip is assumed to be by Knudsen flow<sup>13</sup> at low pressures. The rates of hydrogen diffusion and embrittlement were assumed to be much faster than those of gas transport and surface reaction, and, therefore, did not need to be considered.

The governing differential equations for flow and surface reactions, and the relationship for  $(da/dN)_{cf}$  are as follows:<sup>5</sup>

<sup>1/</sup> In the original derivation,<sup>5</sup> it was assumed that only the area produced by the previous cycle of crack growth contributed to embrittlement. It is recognized that a greater portion of the crack surface remained active, particularly for slow surface reactions and at high frequencies, and can contribute hydrogen to the embrittlement process.<sup>8</sup> To provide consistency, while retaining the form of the original model, an "effective" crack area or "effective" crack increment  $\Delta a^*$  is defined here.

$$\frac{dp}{dt} = - \frac{SN_o RT}{V} \frac{d\theta}{dt} + \frac{F}{V}(p_o - p) \quad (2)$$

$$\frac{d\theta}{dt} = k_c p f(\theta) = k_c p (1 - \theta) \quad (3)$$

$$(da/dN)_{cf} \propto \theta \cdot \Delta a^* \frac{1}{\quad} \quad (4)$$

The terms in the equations are as follows:<sup>5</sup>

$F = 8.72 \times 10^2 \beta (\sigma_{ys}/E)^2 (T/M)^{1/2} B\ell$  (in  $m^3/s$ ) =  
Knudsen flow parameter that depends on dimension and shape of the capillary, molecular weight (M) of the gas and temperature (T). The specific form of this expression reflects an attempt to account for constriction in flow by the real crack, where  $\ell$  is a selected distance (of the order  $10^{-6}$  m) from the crack tip used in defining a crack opening and  $\beta$  is an empirical quantity to be determined from the crack growth data.<sup>5,13</sup>

$k_c$  = reaction rate constant;  $(Pa \cdot s)^{-1}$ .

$N_o$  = density of surface sites; molecules (atoms)- $m^{-2}$ .

$p$  = pressure of gas at the crack tip; Pa.

$p_o$  = pressure of gas in the surrounding environment; Pa.

$R$  = gas constant =  $1.38 \times 10^{-23}$  Pa- $m^3$ -molecules $^{-1}$  - K $^{-1}$ .

$S$  = area of "effective" crack surface per cycle =  $\alpha (2B\Delta a^*)$ , where  $\Delta a^*$  = "effective" increment per cycle,  $B$  = specimen thickness, and  $\alpha$  = empirical constant for surface roughness and crack geometry.<sup>5</sup>

$T$  = absolute temperature.

$V$  = control volume at the crack tip, i.e., volume associated with the distance  $\ell$ .

$\theta$  = fractional surface coverage or extent of reaction of surface per unit area.

From eqn. (2), it can be seen that the rate of change of pressure at the crack tip depends on the decrease in pressure produced by reaction of the environment with the active ("effective") crack surface and on the increase in pressure from the influx of gas from the external environment. The form  $f(\theta) = 1 - \theta$  in eqn. (3) incorporates the assumption that the surface reaction is first-order in relation to available surface sites.<sup>4-7</sup>

Solutions for eqns. (2) and (3), with  $f(\theta) = 1 - \theta$ , were obtained for two limiting cases, for  $0 < \theta < 1$ , and were used in

conjunction with eqn. (4) to estimate the influences of key environmental and loading variables on the cycle-dependent component of fatigue crack growth rate, i.e., on  $(da/dN)_{cf}$ .<sup>5</sup>

4

Case I: Transport controlled.

$$\theta \approx \frac{F}{SN_o RT} p_o t \quad \text{for } \frac{SN_o RT k_c}{F} \gg 1 \quad (5)$$

Case II: Surface reaction controlled.

$$\theta \approx 1 - \exp(-k_c p_o t) \quad \text{for } \frac{SN_o RT k_c}{F} \ll 1 \quad (6)$$

In the transport controlled case, because of the rapid reactions of the environment with the freshly created crack surfaces (high  $k_c$ ) and the limited rate of supply of the environment to the crack tip, significant attenuation of gas pressure takes place at the crack tip. The extent of surface reaction ( $\theta$ ) during one cycle is controlled by the rate of transport of the aggressive environment to the crack tip, and thus varies linearly with time (see eqn. (5)). For the surface reaction controlled case, the reaction rates are sufficiently slow so that the gas pressure at the crack tip is essentially equal to the external pressure. The extent of reaction, for  $f(\theta) = 1 - \theta$ , becomes an exponential function of time, eqn. (6).

As a modification to the original model,<sup>5,8</sup> the "effective" crack increment ( $\Delta a^*$ ) is now chosen, along with  $l$  in the expression of  $F$ , to be equal to the growth increment per cycle at saturation (i.e., for  $\theta \approx 1$ ,  $\Delta a^* = l = (da/dN)_{e,s} \cdot 1$ ). By taking  $t$  equal to  $\tau/2$  or  $1/2f$ ,<sup>5,8</sup> the following expressions can be obtained from eqns. (4), (5) and (6):

Case I: Transport controlled.

$$(p_o/2f)_s \approx \frac{SN_o RT}{F} = \left[ 4.36 \times 10^2 \frac{\beta}{\alpha} \frac{\sigma_{ys}^2}{N_o RTE^2} (T/M)^{1/2} \right]^{-1} \quad (7)$$

$$\frac{(da/dN)_{cf}}{(da/dN)_{e,s}} \approx 4.36 \times 10^2 \frac{\beta}{\alpha} \frac{\sigma_{ys}^2}{N_o RTE^2} (T/M)^{1/2} \frac{p_o}{2f} \quad (8)$$

$$\frac{(da/dN)_{cf}}{(da/dN)_{cf,s}} = \frac{(p_o/2f)}{(p_o/2f)_s} \quad (9)$$



Case II: Surface reaction controlled.

$$\frac{(da/dN)_{cf}}{(da/dN)_{e,s}} \propto 1 - \exp(-k_c p_o/2f) \quad (10)$$

$$\frac{(da/dN)_{cf}}{(da/dN)_{cf,s}} = 1 - \exp(-k_c p_o/2f) \quad (11)$$

Subscript *s* is used to denote the corresponding values at saturation. The modification affects only the form of the expressions for the surface reaction controlled case, and provides a physically more acceptable model. In their present form, the model appears to be in excellent agreement with the experimental observations<sup>2/5-9,14</sup>. An example of this correlation is illustrated in Fig. 1 for transport controlled crack growth in a 2219-T851 aluminum alloy.<sup>6</sup>

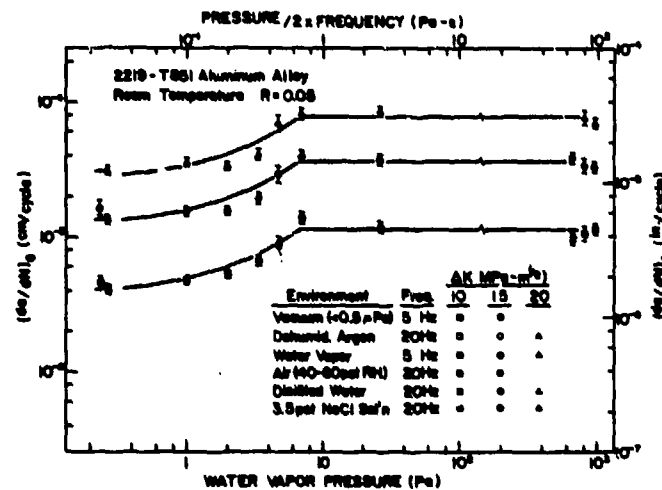


Fig. 1. Influence of water vapor pressure (or pressure/2xfrequency) on fatigue crack growth rates in 2219-T851 aluminum alloy at room temperature. Solid lines represent model predictions.<sup>5,6</sup>

<sup>2/</sup>There is a discrepancy of  $10^2$  in exposure ( $p_o/2f$ ) between the model predictions and the experimental data on AISI 4340 steel,<sup>9</sup> suggesting that capillary condensation of water vapor may have taken place. With capillary condensation, the effective exposure can be much higher than that given by  $p_o/2f$ .

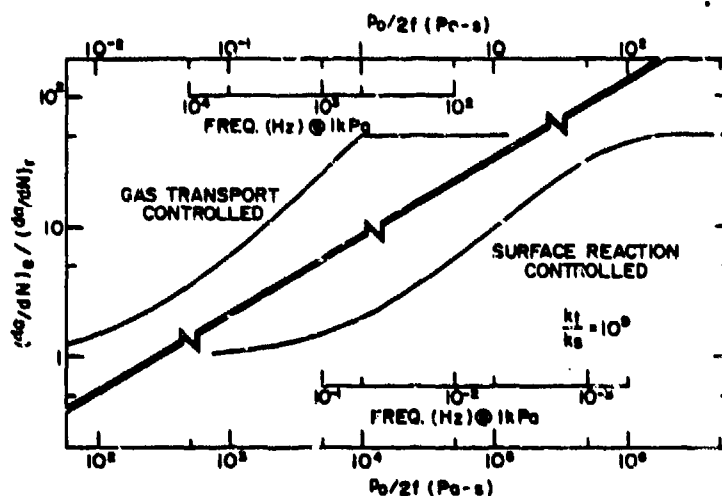


Fig. 2. Schematic illustration and comparison of gas transport and surface reaction controlled fatigue crack growth.

The engineering significance and implications of the model may be discussed in relation to eqns. (7) and (11), and considered through the schematic illustration shown in Fig. 2. The model provides a formalism for "predicting" environmentally assisted fatigue crack growth response in relation to gas pressure and cyclic load frequency. Specifically, eqn. (7) gives, for the transport controlled case, the value of  $p_0/2f$  at which "saturation" in environmental effect can be expected in terms of the properties of the alloy, molecular weight of the aggressive gas, and temperature. Fatigue crack growth response is given, for this case, as an explicit function of  $p_0/2f$  below saturation by eqns. (8) and (9). For the surface reaction controlled case, the dependence of fatigue crack growth response on  $p_0/2f$  is given by eqns. (10) and (11). It should be noted that eqns. (8) to (11) deal only with relative rates. The actual growth rates depend on the interactions of the embrittling specie (hydrogen) with the alloy, which are not adequately understood at this time.

As further illustration, two hypothetical cases -- one representing gas transport and the other surface reaction control -- are shown in Fig. 2. Crack growth response curves are given in terms of the ratio  $(da/dN)_e / (da/dN)_r$ , as functions of  $p_0/2f$ , which can be readily obtained from eqns. (1), (8) and (11). In addition, frequency scales are shown for an external pressure ( $p_0$ ) of 1 kPa. For this illustration,  $(da/dN)_{e,s} / (da/dN)_r = 50$ , and  $k_c = 2 \times 10^3$  and  $2 \times 10^{-6} \text{ (Pa-s)}^{-1}$  are used. Although the curves differ somewhat in detail from experimental data, they do serve to illustrate fatigue crack growth response for a high strength steel exposed to hydrogen

sulfide (transport controlled) and water vapor (reaction controlled).<sup>7</sup> It can be seen that the range of exposures ( $p_0/2f$ ) or frequencies over which apparent frequency dependence may be observed differ by about 6 orders of magnitude for the two cases. The apparent independence of frequency or pressure, or  $p_0/2f$ , does not imply absence of environmental effect. Neither does testing at high frequencies in itself ensure absence of environmental effects. Most importantly, each material-environment system must be considered individually. Generalizations and extrapolations on the basis of limited data can be very misleading and should be avoided.

#### MODELING OF FATIGUE CRACK GROWTH IN BINARY GAS MIXTURE

Experimental evidence obtained to date<sup>1-4,6-9</sup> clearly indicates that the rate of environment assisted crack growth is dependent on the rate of hydrogen production at the crack surfaces. The model for fatigue crack growth developed earlier<sup>5,8</sup> may be readily extended to the consideration of crack growth in gas mixtures. For simplicity, the case of a binary mixture is considered. One of the component gases is taken to be an inhibitor (that is, a gas which will react with the clean metal surface but will not enhance crack growth). As such, the results may be used, for example, to examine the influence of oxygen (an inhibitor) on fatigue crack growth in humid air, where water vapor is the aggressive component.<sup>14-16</sup>

It is assumed that (i) both gases are strongly adsorbed on the clean metal surface, (ii) chemical adsorption of either gas at a given surface site precludes further adsorption at that site, (iii) the ratio of partial pressures of the gases at the crack tip is essentially the same as that of the surrounding environment, and (iv) no capillary condensation of either gas occurs at the crack tip. In line with the model of Weir et al.,<sup>5</sup> the cycle-dependent component of crack growth rate in the gas mixture,  $(da/dN)_{cf,m}$ , is assumed to be proportional to the extent of surface reaction with the aggressive gas during one loading cycle, or to  $\theta_a$ . If one now assumes, for simplicity, that the kinetics of surface reaction for both gases are first order with respect to pressure and to available surface sites, then the rate equations for the surface reactions may be written as follows:

$$\frac{d\theta_a}{dt} = k_a p_a (1 - \theta) \quad (12)$$

$$\frac{d\theta_i}{dt} = k_i p_i (1 - \theta) \quad (13)$$

where the subscripts a and i denote the aggressive and inhibitor gases respectively. The quantities  $k_a$ ,  $p_a$ ,  $k_i$  and  $p_i$  are the

reaction rate constants and partial pressures of the gases at the crack tip, respectively. The coverages  $\theta_a$  and  $\theta_i$  denote the fraction of surface that has reacted with the aggressive and inhibitor gases, respectively. Coverage for both gases is denoted by  $\theta$ , where  $\theta = \theta_a + \theta_i$  and  $0 \leq \theta \leq 1$ .

Eqs. (12) and (13) may be solved straightforwardly to obtain the extent of reaction of a fresh surface with each gas after being exposed to the gas mixture for a time  $t$ .

$$\theta_a = \frac{k_a p_a}{k_a p_a + k_i p_i} [1 - \exp[-(k_a p_a + k_i p_i)t]] \quad (14)$$

$$\theta_i = \frac{k_i p_i}{k_a p_a + k_i p_i} [1 - \exp[-(k_a p_a + k_i p_i)t]] \quad (15)$$

It follows that the fraction of surface that has reacted with the aggressive gas ( $\theta_a$ ) in relation to the total surface coverage ( $\theta$ ) may be given by eqn. (16).

$$\frac{\theta_a}{\theta} = \frac{\theta_a}{\theta_a + \theta_i} = \left(1 + \frac{k_i p_i}{k_a p_a}\right)^{-1} \quad (16)$$

If the total pressure of the gas mixture at the crack tip ( $p_m = p_a + p_i$ ) and cyclic-load frequency, or  $p_m/2f$ , are such to produce "complete" surface reaction or "saturation" coverage ( $\theta \approx 1$ ) during one cycle, then the fraction of the crack surface that has reacted with the aggressive gas is given by eqn. (17).

$$\theta_a = \left(1 + \frac{k_i p_i}{k_a p_a}\right)^{-1} ; \quad (\theta \approx 1) \quad (17)$$

Since  $(da/dN)_{cf} \propto \theta \cdot \Delta a^*$  (see eqn. (4)), the cycle-dependent component of fatigue crack growth rate in the mixed gases,  $(da/dN)_{cf,m}$ , can be obtained from the cycle-dependent rate in a pure gas at saturation,  $(da/dN)_{cf,p,s}$ , and eqn. (17).

$$\frac{(da/dN)_{cf,m}}{(da/dN)_{cf,p,s}} = \left(1 + \frac{k_i p_i}{k_a p_a}\right)^{-1} = \left(1 + \frac{k_i p_{io}}{k_a p_{ao}}\right)^{-1} \quad (18)$$

(for  $\theta \approx 1$ )

The subscript o is used to denote pressures in the external environment, and reflects the assumption that the partial pressure ratio at the crack tip is the same as that in the external environment. It should be noted that only the competition between two gases has been modeled here, and eqn. (18) is expected to apply equally well to both transport and surface reaction controlled crack growth. Schematic illustration of eqn. (18) is shown in Fig. 3 as  $(da/dN)_{e,m}/(da/dN)_r$  for different ratios of  $(da/dN)_{e,s}/(da/dN)_r$ ; the ratios reflect different degrees of severity of environmental effects in the pure gas. A ratio of  $k_1/k_2$  of 0.14, which approximates the ratio between the reaction rate constants for oxygen and water vapor over a 2219-T851 aluminum alloy,<sup>6,17</sup> is used. The upper scale for  $p_a$  in Fig. 3 is computed for  $p_i = 152$  torr (or 20.2 kPa), and therefore corresponds to the partial pressure of water vapor in humid (moist) air.

Assuming that the surface reaction data on 2219-T851 aluminum alloys<sup>6,17</sup> may be used for other high-strength aluminum alloys, comparisons of model predictions with data reported by Hartman et al.<sup>15</sup> and Feeney, McMillan and Wei<sup>16</sup> on 7075-T6 aluminum alloy, and Bradshaw and Wheeler<sup>14</sup> on DTD 5070A aluminum alloy are made and are shown in Figs. 4 and 5, respectively. For the 7075-T6 aluminum alloy, data in water and salt water<sup>16</sup> are assumed to represent the "saturation" level in pure water vapor ( $\theta = 1$ ).<sup>6</sup> Excellent agreement is observed at the higher K levels and higher crack growth rates. At the lower K levels and lower crack growth rates, the data tend to follow those of pure water vapor, and may reflect partial capillary condensation during a portion of each loading-unloading

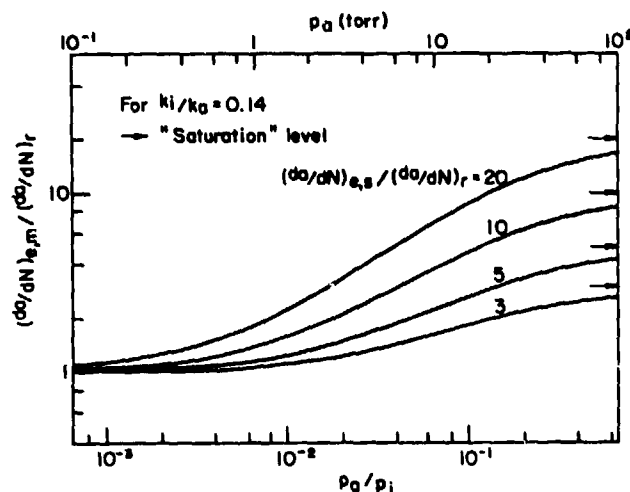


Fig. 3. Schematic illustration of the influence of inhibitor gas on fatigue crack growth in a binary gas mixture. (In the upper scale,  $p_a$  corresponds to  $p_i = 152$  torr or 20.2 kPa.)

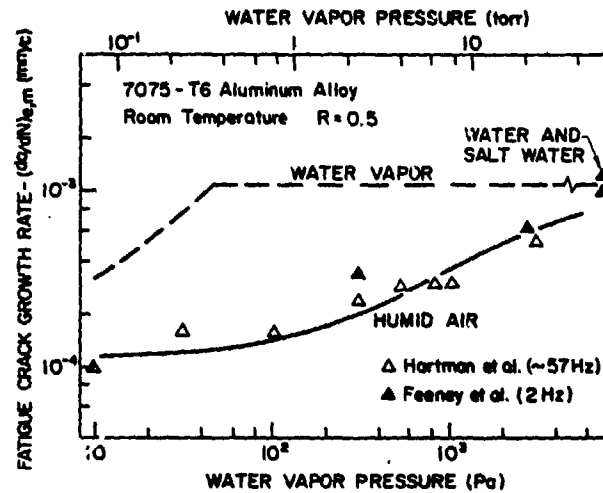


Fig. 4. Influence of water vapor pressure on fatigue crack growth in 7075-T6 aluminum alloy in humid air.<sup>15,16</sup> Dashed and solid lines represent model predictions from eqns. (7), (8) and (18).

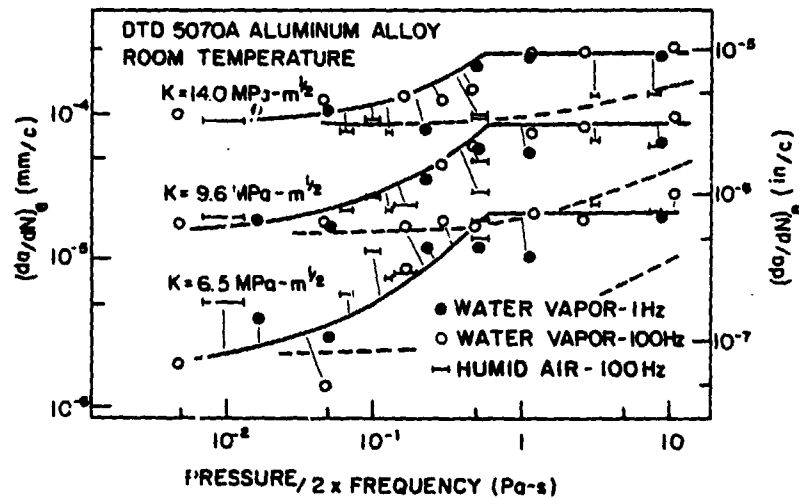


Fig. 5. Influence of water vapor pressure and frequency on fatigue crack growth in DTD 5070A aluminum alloy.<sup>14</sup> Solid lines represent model predictions for water vapor, and dashed lines for humid air.

cycle or some other factor. Further studies are needed to clarify this discrepancy.

## DISCUSSION

On the basis of available experimental results, it is seen that the models reasonably account for environmentally assisted fatigue crack growth response in single-component gaseous environments and in binary gas mixtures, in which one of the components acts as an inhibitor. A similar consideration of environmentally assisted crack growth in binary gas mixtures, under sustained loading, has also been made and provided good agreement with experimental observations.<sup>18</sup> Thus, the models provide a formalism for the planning of experiments, and for the interpretation and extrapolation of data for engineering applications.

In deriving these models and in their application, only simple surface reactions have been considered. Many reactions that are of interest (for example, reactions of steels with water vapor or hydrogen sulfide), however, are more complex. Reactions of different components to form new complexes are also possible. Incorporation of these complexities into future modeling efforts must be considered. Extension of these ideas to the consideration of fatigue crack growth in mixtures of  $H_2S$  and  $CO$  has been made.<sup>19,20</sup> Preliminary results indicate that modeling of the more complex environments would be feasible.

## SUMMARY

Based on considerations of surface reactions and gas transport, models of environmentally assisted fatigue crack growth in single-component gaseous environments and in binary gas mixtures (in which one of the components acts as an inhibitor) have been developed. Good agreement with experimental data has been observed. The models, therefore, provide a formalized framework for experimental design, and for the interpretation and extrapolation of data for engineering applications. Further research will be needed to refine and extend this work to the consideration of more complex environments, and to incorporate the influences of metallurgical variables.

## ACKNOWLEDGEMENT

Partial support of this work by the Office of Naval Research under Contract N00014-75-C-0543, NR 036-097 is gratefully acknowledged.

## REFERENCES

1. G. W. Simmons, P. S. Pao, and R. P. Wei, Met. Trans. A 9A:1147 (1978).

2. M. Lu, P. S. Pao, N. H. Chan, K. Klier, and R. P. Wei, in: "Hydrogen in Metals", Suppl. to Trans. Japan Inst. Metals 21:449 (1980).
3. N. H. Chan, K. Klier, and R. P. Wei, in: "Hydrogen in Metals", Suppl. to Trans. Japan Inst. Metals 21:305 (1980).
4. M. Lu, P. S. Pao, T. W. Weir, G. W. Simmons, and R. P. Wei, Rate Controlling Processes for Crack Growth in Hydrogel Sulfide for an AISI 4340 Steel, submitted for publication to Met. Trans. A (1980).
5. T. W. Weir, G. W. Simmons, R. G. Hart, and R. P. Wei, Scripta Met. 14:357 (1980).
6. R. P. Wei, P. S. Pao, R. G. Hart, T. W. Weir, and G. W. Simmons, Met. Trans. A 11A:151 (1980).
7. R. L. Brazill, G. W. Simmons, and R. P. Wei, J. Engr. Matls. & Tech., Trans. ASME 101:199 (1979).
8. R. P. Wei and G. W. Simmons, Recent Progress in Understanding Environment Assisted Fatigue Crack Growth, Int. J. Fract. (to be published) (1980).
9. P. S. Pao, W. Wei, and R. P. Wei, in: "Environment Sensitive Fracture of Engineering Materials", Z. A. Foroulis, ed., TMS-AIME, New York:565 (1979).
10. R. P. Wei, in: ASTM STP 675 "Fatigue Mechanisms", J. T. Fong, ed., Am. Soc. Testing Matls., Philadelphia:816 (1979).
11. J. D. Landes and R. P. Wei, J. Engr. Matls. & Tech., 95:2 (1973).
12. G. A. Miller, S. J. Hudak, and R. P. Wei, J. Testing & Eval., ASTM 1:524 (1973).
13. S. Dushman, "Scientific Foundations of Vacuum Techniques", 2nd ed., J. M. Lafferty, ed., Wiley:88 (1962).
14. F. J. Bradshaw and C. Wheeler, RAE Tech. Rept. No. 68041, England (1968).
15. A. Hartman, F. J. Jacobs, A. Nederveen, and R. DeRijk, NLR Tech. Note No. M.2182, The Netherlands (1967).
16. J. A. Feeney, J. C. McMillan, and R. P. Wei, Met. Trans. 1:1741 (1970).
17. R. G. Hart, G. W. Simmons, and R. P. Wei, Studies of the Reaction of Oxygen and Water Vapor With 2219-T851 Aluminum Alloy, submitted for publication to J. Electrochem. (1980).
18. R. P. Wei, Rate Controlling Processes and Crack Growth Response, prepared for the 3rd Intl. Conf. on Effect of Hydrogen on Behavior of Materials, Jackson Lake Lodge, Wyoming, Aug. 26-31, 1980.
19. R. P. Wei and G. W. Simmons, Fracture Mechanics and Surface Chemistry Studies of Steels for Coal Gasification Systems, Final Tech. Rept., Contract No. Ex-76-S-01-2527, DOE-Fossil Energy Research, Lehigh University, Bethlehem, PA (1980).
20. R. L. Brazill, G. W. Simmons, and R. P. Wei, unpublished results, Lehigh University, Bethlehem, PA (1980).



# BASIC DISTRIBUTION LIST

Technical and Summary Reports

April 1978

<u>Organization</u>	<u>Copies</u>	<u>Organization</u>	<u>Copies</u>
Defense Documentation Center Cameron Station Alexandria, VA 22314	12	Naval Air Propulsion Test Center Trenton, NJ 08628 ATTN: Library	1
Office of Naval Research Department of the Navy 800 N. Quincy Street Arlington, VA 22217		Naval Construction Battalion Civil Engineering Laboratory Port Hueneme, CA 93043 ATTN: Materials Division	1
ATTN: Code 471	1	Naval Electronics Laboratory San Diego, CA 92152 ATTN: Electron Materials Sciences Division	1
Code 102	1		
Code 470	1		
Commanding Officer Office of Naval Research Branch Office Building 114, Section D 666 Summer Street Boston, MA 02210	1	Naval Missile Center Materials Consultant Code 3312-1 Point Mugu, CA 92041	1
Commanding Officer Office of Naval Research Branch Office 536 South Clark Street Chicago, IL 60605	1	Commanding Officer Naval Surface Weapons Center White Oak Laboratory Silver Spring, MD 20910 ATTN: Library	1
Office of Naval Research San Francisco Area Office One Hallidie Plaza Suite 601 San Francisco, CA 94102	1	David W. Taylor Naval Ship Research and Development Center Materials Department Annapolis, MD 21402	1
Naval Research Laboratory Washington, DC 20375		Naval Undersea Center San Diego, CA 92132 ATTN: Library	1
ATTN: Codes 6000	1	Naval Underwater System Center Newport, RI 02840 ATTN: Library	1
6100	1		
6300	1		
6400	1		
2627	1	Naval Weapons Center China Lake, CA 93555 ATTN: Library	1
Naval Air Development Center Code 382 Warminster, PA 18964 ATTN: Mr. F. S. Williams	1	Naval Postgraduate School Monterey, CA 93940 ATTN: Mechanical Engineering Department	1

# BASIC DISTRIBUTION LIST (cont'd)

<u>Organization</u>	<u>Copies</u>	<u>Organization</u>	<u>Copies</u>
Naval Air Systems Command Washington, DC 20360 ATTN: Codes 52031 52032	1	NASA Headquarters Washington, DC 20546 ATTN: Code:RRM	1
Naval Sea System Command Washington, DC 20362 ATTN: Code 035	1	NASA Lewis Research Center 21000 Brookpark Road Cleveland, OH 44135 ATTN: Library	1
Naval Facilities Engineering Command Alexandria, VA 22331 ATTN: Code 03	1	National Bureau of Standards Washington, DC 20234 ATTN: Metallurgy Division Inorganic Materials Div.	1 1
Scientific Advisor Commandant of the Marine Corps Washington, DC 20380 ATTN: Code AX	1	Director Applied Physics Laboratory University of Washington 1013 Northeast Fortthieth Street Seattle, WA 98105	1
Naval Ship Engineering Center Department of the Navy Washington, DC 20360 ATTN: Code 6101	1	Defense Metals and Ceramics Information Center Battelle Memorial Institute 505 King Avenue Columbus, OH 43201	1
Army Research Office P.O. Box 12211 Triangle Park, NC 27709 ATTN: Metallurgy & Ceramics Program	1	Metals and Ceramics Division Oak Ridge National Laboratory P.O. Box X Oak Ridge, TN 37380	1
Army Materials and Mechanics Research Center Watertown, MA 02172 ATTN: Research Programs Office	1	Los Alamos Scientific Laboratory P.O. Box 1663 Los Alamos, NM 87544 ATTN: Report Librarian	1
Air Force Office of Scientific Research Bldg. 410 Bolling Air Force Base Washington, DC 20332 ATTN: Chemical Science Directorate Electronics & Solid State Sciences Directorate	1 1	Argonne National Laboratory Metallurgy Division P.O. Box 229 Lemont, IL 60439	1
Air Force Materials Laboratory Wright-Patterson AFB Dayton, OH 45433	1	Brookhaven National Laboratory Technical Information Division Upton, Long Island New York 11973 ATTN: Research Library	1
Library Building 50, Rm 134 Lawrence Radiation Laboratory Berkeley, CA	1	Office of Naval Research Branch Office 1030 East Green Street Pasadena, CA 91106	1

**DISTRIBUTION LIST**  
**Corrosion Mechanisms**

Professor J. P. Hirth  
Ohio State University  
Department of Metallurgical Engineering  
1314 Kinnear Road  
Columbus, OH 43212

Dr. J. Kruger  
National Bureau of Standards  
Washington, DC 20234

Dr. H. K. Birnbaum  
University of Illinois  
Department of Metallurgy and Mining Engineering  
Urbana, IL 61801

Dr. D. J. Duquette  
Rensselaer Polytechnic Institute  
Department of Metallurgical Engineering  
Troy, NY 12181

Dr. R. P. Wei  
Lehigh University  
Institute for Fracture and Solid Mechanics  
Bethlehem, PA 18015

Prof. H. W. Pickering  
Pennsylvania State University  
Department of Material Science  
University Park, PA 16802

Prof. I. M. Bernstein  
Carnegi-Mellon University  
Schenley Park  
Pittsburg, PA 15213

Dr. T. R. Beck  
Electrochemical Technology Corporation  
10035 31st Avenue, N.E.  
Seattle, WA 98125

Prof. R. T. Foley  
The American University  
Washington, DC 20016

Dr. D. L. Davidson  
Southwest Research Institute  
8500 Culebra Road  
P.O. Box Drawer 28510  
San Antonio, TX 78284

Dr. Barry C. Syrett  
Stanford Research Institute  
333 Ravenswood Avenue  
Menlo Park, CA 94025

Prof. S. Weissmann  
Rutgers, The State University  
of New Jersey  
College of Engineering  
New Brunswick, NY 08903

Prof. H. Herman  
State University of New York  
Material Science Department  
Stony Brook, NY 11794

Prof. R. M. Latanision  
Massachusetts Institute of  
Technology  
77 Massachusetts Avenue, Room E19-702  
Cambridge, MA 02139

Prof. E. A. Starke, Jr.  
Georgia Institute of Technology  
School of Chemical Engineering  
Atlanta, GA 30332

Prof. Morris E. Fine  
Northwestern University  
The Technological Institute  
Evanston, IL 60201

Dr. C. S. Kortovich  
TRW, Inc.  
2355 Euclid Avenue  
Cleveland, OH 44117

Dr. O. Buck  
Rockwell International Science Center  
1049 Camino Dos Rios  
P.O. Box 1085  
Thousand Oaks, CA 91360

Dr. R. J. Arsenault  
University of Maryland  
College Park, MD 20742

Dr. F. Mansfeld  
Rockwell International (Science Ctr)  
1049 Camino Dos Rios  
P.O. Box 1085  
Thousand Oaks, CA 91360

Continue of Distribution List

036  
16 November 1981

Dr. Paul Gordon  
Illinois Institute of Technology  
Department of Metallurgical and Materials  
Engineering  
Chicago, IL 60616

Dr. Theodore R. Beck  
Electrochemical Technology Corp.  
3935 Leary Way NW  
Seattle, Washington 98107

Dr. H. Leidheiser, Jr.  
Lehigh University  
Bethlehem, PA 18015

Dr. J. V. McArdle  
University of Maryland  
College Park, MD 20742

Br. E. McCafferty  
Naval Research Laboratory  
Washington, DC 20375

Prof. J. G. Byrne  
The University of Utah  
Dept. of Materials Science & Engineering  
Salt Lake City, Utah 84112

Prof. A. J. Ardell  
University of California  
School of Engineering and Applied Science  
405 Hilgard Ave.  
Los Angeles, CA 90024

Prof. J. A. S. Green  
Martin Marietta Corporation  
1450 South Rolling Road  
Baltimore, MD 21227

Prof. G.H. Meier & F.S. Pettit  
University of Pittsburgh  
Dept. of Metallurgical and Materials  
Engineering  
Pittsburgh, PA 15261

Prof. Alexander M. Cruickshank  
Gordon Research Conference  
Pastore Chemical Laboratory  
University of Rhode Island  
Kingston, RI 02881